BIOCHEMICAL AND BIOPHYSICAL RESEARCH COMMUNICATIONS **243,** 41–46 (1998)
ARTICLE NO. RC978054

Pseudo-Noncompetitive Antagonism of M_1, M_3, and M_5 Muscarinic Receptor-Mediated Ca^{2+} Mobilization by Muscarinic Antagonists

Jyrki P. Kukkonen,*,†,[1] Johnny Näsman,*,† Ago Rinken,‡
Anton Dementjev,‡ and Karl E. O. Åkerman*

**Department of Physiology and Medical Biophysics, Uppsala University, Uppsala, Sweden; †Department of Biochemistry and Pharmacy, Åbo Akademi University, Turku, Finland; and ‡Institute of Chemical Physics, University of Tartu, Tartu, Estonia*

Received December 19, 1997

Muscarinic receptors M_1, M_3 and M_5 were expressed in Sf9 cells. Three different patterns of inhibition of Ca^{2+} elevations could be resolved for the subtype nonselective muscarinic receptor antagonists: (i) a right shift of the agonist dose-response curve, (ii) a right shift of the agonist dose-response curve and a depression of the maximum signal, and (iii) an intermediate pattern where the antagonist apparently behaved more competitively at higher concentrations. A simulation performed assuming that these differences are due to differences in the dissociation rates of the antagonists reproduced all three different modes of inhibition; the novel intermediate pattern (iii) is suggested to be caused by an intermediate antagonist dissociation rate. A direct correlation between the type of inhibition and the measured dissociation rate of the antagonists was also observed. Functional selectivity between receptor subtypes based on the dissociation constants is suggested based on the results. © 1998 Academic Press

Many G protein coupled receptor antagonists, known to be competitive in binding studies, display an apparent noncompetitive inhibition of agonist-induced signals (1-10). This has been suggested to be due to the slow dissociation of the antagonist from the receptor (1, 2, 10, 11). Such a mechanism may thus affect all fast or transient responses mediated by receptors. Because of its kinetic character this type of inhibition has been called pseudo-noncompetitive (2) or insurmountable (11). Ca^{2+} elevation is the best known rapid and transient second-messenger signal due to a rapid of IP_3 production and Ca^{2+} store depletion as well as and removal of Ca^{2+} from the cytosol. Consequently, an apparent noncompetitive inhibition has been observed in muscarinic receptor mediated Ca^{2+} and IP_3 responses (1-4). previous results have suggested that pseudo-noncompetitive antagonist may show receptor subtype selectivity (7). We have therefore in this study aimed to scrutinize these previous observations by comparing the effects of three different muscarinic receptor antagonists on three different muscarinic receptors coupled to Ca^{2+} elevation. Of the previously investigated antagonists only those displaying no subtype selectivity in terms of binding affinity – NMS, atropine, 4-DAMP – were chosen. To avoid any tissue differences the study was performed using cloned human muscarinic receptors heterologously expressed in Sf9 cells using the baculovirus expression vector system (12).

MATERIALS AND METHODS

All the methods and materials used except the assay of binding kinetics are essentially the same as in (12). Briefly, Spodoptera frugiperda (Sf9) cells were grown in TNMFH medium (pH 6.3, 9 mM $CaCl_2$) supplemented with penicillin, streptomycin, amphotericin B and fetal calf serum in larger scale in suspension at 25°C using glass spinner bottles.

Ca^{2+} measurements. The cells were plated out on plastic culture dishes (∅60 or 94 mm; Greiner, Germany), infected, adaptated to pH 7.4, loaded with fura-2, and the Ca^{2+} measured and calculated as described in (12). The antagonists were added 5 min prior to the addition of carbachol. As calculated from the association rates, this time was enough for 4-DAMP but not for NMS to reach a complete occupation. Because longer antagonist incubation times were not

[1] To whom correspondence should be addressed at Department of Physiology and Medical Biophysics, Uppsala University, BMC, P.O. Box 572, S-75123 Uppsala, Sweden. Fax: +46-18-471 4938/4423. E-mail: jkukkone@fysiologi.uu.se.

Abbreviations: 4-DAMP, 4-diphenylacetoxy-N-metylpiperidine methiodide; HBM, Hepes buffered medium; K_d, the antagonist dissociation constant; K_i, the competitive inhibition constant; K_i', the noncompetitive inhibition constant; k_{off}, the measured antagonist dissociation rate; mAChR, muscarinic acetylcholine receptor; NMS, N-methyl scopolamine; $t_{1/2}$, the antagonist dissociation half-time.

0006-291X/98 $25.00

practically possible, the association and dissociation rate constants were used to calculate the actual receptor occupancies, and the antagonist concentrations these would correspond to if the reaction was in equilibrium.

Binding experiments with intact cells. The cells were cultured, infected and detached as for the Ca^{2+} measurements. They were washed once and suspended in 300 μl HBM with 4.5 nM [^{3}H]NMS (90-100% saturation was obtained with this concentration) ± 10 μM atropine to determine the non-specific binding. Reactions were allowed to proceed for 120 min at 22°C, a time in which binding reached the maximum level. Reactions were terminated by rapid filtration through glass fiber filters with subsequent 4 washes with ice-cold HBM, the filters were dried and the radioactivity counted.

Kinetic binding experiments. The cells used in experiments were grown in glass spinner bottles and infected with respective recombinant virus with a multiplicity of infection of about 1. 48 h post infection the cells were spun down, washed twice with phosphate buffered saline, and frozen down at −80°C. Cells were homogenized with a Potter-type teflon homogenizer in homogenization buffer (50 mM Tris-HCl, 5 mM EDTA, 1 mM EGTA, 0.1 mM phenylmethylsulfonyl fluoride, 0.5 μg/ml pepstatin A, 0.2 mM benzamidine, pH 7.4) and centrifuged for 40 min at 30 000 × *g*. Homogenization and centrifugation were repeated and the final pellets homogenized in incubation buffer (20 mM K^+-Hepes, 100 mM NaCl, 5 mM $MgCl_2$, 1 mM EDTA, pH 7.4) and stored at −80°C.

In the ligand association kinetic experiments the homogenate was incubated at 25°C and reaction was initiated by the addition of the radioligand (1.5 nM [^{3}H]NMS or 5 nM [^{3}H]4-DAMP). At the time *t*, aliquots of the reaction mixture were taken and the reactions were terminated and free ligand removed by fast filtration through glass fiber filters, presoaked in 0.3% polyethylenimine. The filters were washed, dried and the radioactivity determined by scintillation counting. Protein concentrations were determined by the modified Lowry method (13) using BSA as standard. 1 μM atropine was used to determine the nonspecific binding.

The dissociation kinetics of the receptor-radioligand-complex were determined after preincubation of the homogenate with the radioligands for 60 min at 25°C. The dissociation was initiated by addition of atropine (final concentration 1 μM) or carbachol (10 mM), and at the time *t*, aliquots of the reaction mixture were taken and the specifically bound radioactivity was determined as described above.

Drugs. Atropine sulfate, BSA, carbamylcholine chloride (carbachol, CCh) and EGTA were purchased from Sigma Chemical Co. (St. Louis, MO). 4-DAMP and NMS were from RBI (Natick, MA) and fura-2 acetoxymethyl ester from Molecular Probes (Eugene, OR). [^{3}H]4-DAMP (75.4 Ci/mmol) and [^{3}H]NMS (79.5 or 84 Ci/mmol) were purchased from DuPont NEN (Boston, MA).

Mathematics. The equation for linear mixed inhibition (14) describes inhibition of an enzyme with an inhibitor binding both to the substrate site and to an allosteric site with different affinities under steady-state conditions. Although developed to describe a completely different phenomenon, this equation gives comparable measures describing both the right-shift of the dose-response curve (K_i) and the depression of the maximum signal (K_i'), and it has thus been shown to be useful in the analysis of the antagonistic effects (7).

$$\Delta[Ca^{2+}] = \frac{[A] \times \Delta[Ca^{2+}]_{max}}{[A] \times (1 + [I]/K_i')) + EC_{50} \times (1 + ([I]/K_i))} \qquad [1]$$

$\Delta[Ca^{2+}]$ is the $[Ca^{2+}]_{basal}$ subtracted from $[Ca^{2+}]$; $\Delta[Ca^{2+}]_{max}$ is the maximum Ca^{2+} increase; [A] and [I] the concentrations of the agonist and the antagonist, respectively; EC_{50} the [A] producing half-maximal stimulation; K_i and K_i' the competitive and the noncompetitive inhibition constants, respectively. The non-linear least square curve fitting was performed using SigmaPlot for Windows (Jandel Scientific, Corte Madera, CA) or GraphPad PRISM (GraphPad Software Inc., San Diego, CA).

In order to understand the different modes of inhibition, a simple kinetic model according to the receptor-inactivation theory (15, 16) was constructed. This model was developed to explain signal decay in a mechanistically more likely way than the rate theory (17) does. Actually, the model of becomes formally identical to the receptor occupation theory whenever $k_{-1} \gg k_2 \ll k_3$, and to the rate theory (17), whenever $k_{-1} \ll k_2 \gg k_3$ (15, 16).

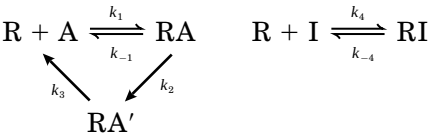

[2]

In this model, R is the receptor, A the agonist and I the antagonist. As the reactions R + A ⊂ RA and R + I ⊂ RI would reach an equilibrium and no apparent noncompetitivity would be observed, an additional step from RA, which is the "active" receptor (representing the signal), to RA′, which is an inactive conformation (representing a conformation of the receptor which is uncoupled from the G protein e.g. the low affinity form of the receptor or the desensitized state), was included. This way of including irreversibility of interaction was used in order to keep the model as simple as possible. In reality the irreversibility of the response is probably in the most cases dependent on the activation Ca^{2+} outpumping. For the describing of the response amplification, the active complex [RA] was taken as the "agonist" in the hyperbolic function

$$\text{response} = \frac{[RA] \times \text{response}_{max}}{[RA] + K_s} \qquad [3]$$

and the maximum obtainable agonist signal was normalized to 100%. This simplified model was numerically integrated over time with different hypothetical forward and reverse rate constants using the freeware Gepasi 2.08 (18).

RESULTS

M_1, M_3 and M_5 muscarinic receptor subtypes coupled to Ca^{2+} increase when heterologously expressed in Sf9 insect cells (12). This response was optimal 27-28 h post infection; shorter infection times resulted in a weaker signal and longer infection times in a high basal Ca^{2+} and a large variability in signals, probably due to general adverse effects of the infection. At this time the expression levels were 83.2 ± 32.9, 117.7 ± 60.3 and 36.6 ± 26.8 fmol/mg protein, respectively (mean ± SEM of three determinations) and the corresponding EC_{50}-values for carbachol-induced Ca^{2+} elevation of 7.36 ± 0.54, 5.07 ± 0.30 and 1.98 ± 0.20 μM, respectively (number of determinations = 25-26) . A typical fura-2 fluorescence recording of cells expressing the Hm3 receptor is shown in Fig. 1A. When high concentrations of carbachol (sufficient to completely displace the antagonists from the receptor under equilibrium conditions) were added to Hm3-expressing cells preincubated with atropine, the Ca^{2+} response was clearly biphasic with a fast initial phase followed by a slow increase in the signal. The control value was reached

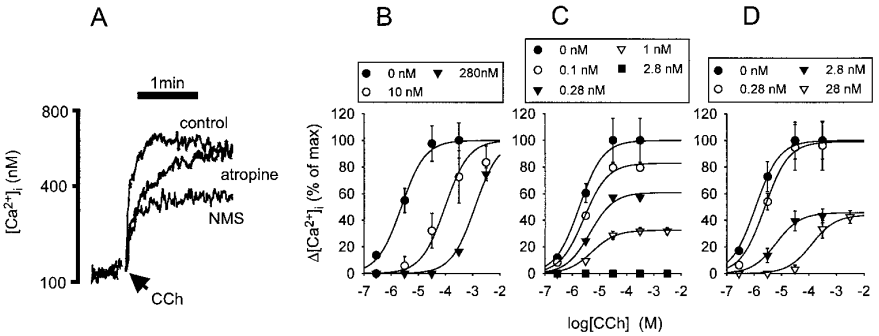

FIG 1. In **A** The effect of different antagonists on carbachol (2.8 mM) induced Ca^{2+} elevation shown as three representative experiments performed with Sf9 cells expressing Hm3 receptors. The uppermost trace is control (no antagonist present), the middle trace is performed in the presence of 10 nM atropine and the lowermost trace in the presence of 1 nM NMS. In **B**, **C** and **D** the three observed patterns of inhibition presented with different antagonists on Sf9 cells expressing Hm5 receptors. Each data point is mean ± SEM from at least two determinations from two independent infections. The antagonist concentrations are indicated in the picture. The NMS concentrations in **B** are not corrected.

approximately in 1-2 min compared to the about 30 s in the absence of atropine. In the presence of NMS only a fast phase of the response could be seen and the $\Delta[Ca^{2+}]_{max}$ value of the control trace was not reached during the time span of the experiment. The faster phase of the signal in the presence of the antagonist may thus represent the binding of the agonist to the free receptor population and the slow phase competition with (and displacement of) the antagonist. NMS would thus be markedly slower displaced from Hm3 receptors than atropine.

When the effects of the three different antagonists (4-DAMP, NMS and atropine) were tested on the carbachol dose-response curves, they were observed to inhibit the carbachol induced Ca^{2+} elevation in different ways with respect to the right-shift of the dose-response curve and the depression of the maximum signal. Three different patterns could be separated (Table 1). In addition to *apparent competitive inhibition* (right-shift of the dose-response curve without a depression of the maximum signal; Fig. 1B; see also (10)) and *apparent noncompetitive inhibition* (a right-shift of the dose-response curve and a depression of the maximum signal; Fig. 1C; see also (7, 10)) a third type of inhibition—here referred to as *apparent partial noncompetitive inhibition*—was observed (Fig. 1D, Table 1). The K_i and K_i' values calculated using the equation for linear mixed inhibition (7, 14) for the first two types of inhibition were independent of antagonist concentration (Table 1) and the Schild plots linear with slopes of unity or more, respectively. The analysis of the third pattern of inhibition resulted in decreasing K_i and increasing K_i' values when the antagonist concentration was increased i.e. the apparent competitivity of the antagonistic effect increased with increasing antagonist concentration (Figs. 1D and 2A). The different effects of the antagonist are likely to be caused by a true effect on the muscarinic receptors as the octopamine (1 mM; endogenous octopamine receptor (19) agonist) and thap-

TABLE 1

The Apparent Modes of Inhibition of Carbachol Induced Ca^{2+} Increase by Different Antagonists

Antagonist	Receptor	Apparent type of inhibition	K_i (nM)	K_i' (nM)
NMS	M_1	Partial noncompetitive	—	—
	M_3	Partial noncompetitive	—	—
	M_5	Noncompetitive	0.0126 ± 0.0017	0.0398 ± 0.0041
Atropine	M_1	Partial noncompetitive	—	—
	M_3	Competitive	0.111 ± 0.026	—
	M_5	Partial noncompetitive	—	—
4-DAMP	M_1	Competitive	0.369 ± 0.056	—
	M_3	Competitive	0.242 ± 0.034	—
	M_5	Competitive	0.645 ± 0.092	—

Note. In the cases where the K_i and/or K_i' could be calculated (*apparent competitive* and *noncompetitive* inhibition), they are indicated. The values are mean ± SEM of 14-18 determinations.

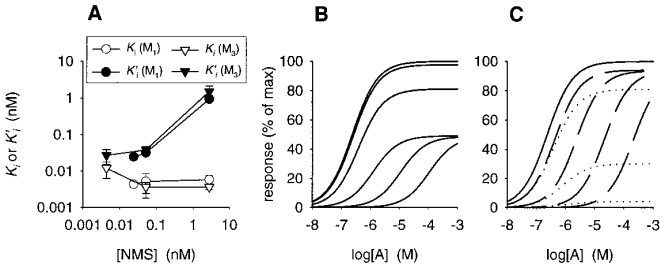

FIG. 2. The apparent *partial noncompetitive inhibition*. In **A** the dependence of K_i and K_i' of [antagonist] exemplified by the behaviour of NMS in Sf9 cells expressing M_1 or M_3 receptors. The values are given as mean ± SEM of at least two determinations. The concentrations of NMS have been corrected as described under Materials and Methods. In **B** and **C** the dose-response curves simulated using Gepasi 2.08 (18). The antagonist was assumed to have reached an equilibrium with the receptor population whereafter the agonist would have been added. In **B** the rate constants for the agonist are $k_1 = 10^6$ $M^{-1}s^{-1}$, $k_{-1} = 1$ s^{-1}, $k_2 = 0.01$ s^{-1}, $k_3 = 10^{-5}$ s^{-1}, and for the antagonist $k_4=3\times10^6$ $M^{-1}s^{-1}$ and $k_{-4}=3\times10^{-3}$ s^{-1}. The dissociation curves were generated and then amplified according to the equation 3 (K_s=30%). The different antagonist concentrations are 0, 0.1, 1, 10, 100, and 1000 nM. In **C** the agonist rate constants are kept the same but the antagonist association and dissociation rate constants varied: dotted lines: $k_4=1\times10^5$ $M^{-1}s^{-1}$ and $k_{-4}=1\times10^{-4}$ s^{-1}, antagonist concentrations shown 1 nM, 10 nM, and 100 nM; dashed lines: $k_4=1\times10^8$ $M^{-1}s^{-1}$ and $k_{-4}=1\times10^{-1}$ s^{-1}, antagonist concentrations shown 1 nM, 10 nM, 100 nM, and 1000 nM. The solid line represents agonist in the absence of the antagonist.

sigargin (1 μM; endoplasmic reticulum Ca^{2+}-ATPase inhibitor) -induced Ca^{2+} elevations were not affected by any of these compounds (data not shown).

The first two patterns would be expected to be caused by fast and slowly dissociating antagonists (7, 10), respectively, but the third pattern is reminiscent of allocteric modulation. Computer simulations were used to see if also the third pattern could be obtained by changing the antagonist dissociation rate constants. Carbachol dose-response curves were created for different antagonist concentrations. The equilibrium constant for antagonist binding was kept constant (= 1 nM) but the on- and off-rate constants of receptor-antagonist-complex formation (k_4 *and* k_{-4}, respectively, in equation (2)) were varied. A low degree of amplification was chosen (K_s=30%) as there was no indication of receptor reserve (i.e. apparent competitive inhibition at low antagonist concentrations and noncompetitive at higher). If the dissociation kinetics of an antagonist are slow enough the dissociation from the receptor before the time in which the maximum stimulation occurs (before "decline") is negligible resulting in apparently noncompetitive inhibition. With increasing on- and off-rates the apparent type of inhibition goes from *noncompetitive* (Fig. 2C, dotted lines) to *partial noncompetitive* (Fig. 2B) and further to *competitive* (Fig. 2C, dashed lines).

The dissociation rates of [^{3}H]NMS and [^{3}H]4-DAMP ([^{3}H]atropine is not commercially available anymore) were also measured. The association and dissociation reactions were first order reactions, i.e. there was no manifestation of allosteric effects or co-operativity. 4-DAMP was shown to dissociate more than 10 times faster from all the receptor subtypes than NMS (Table 2). The dissociation rate did not depend on whether agonist (carbachol) or antagonist (atropine) was used to initiate the dissociation (data not shown); also, a complete displacement was obtained with both. Comparison between receptor subtypes indicated significantly slower ($p < 0.05$) dissociation of both radioligands from M_5-subtype than from subtypes M_1 or M_3. This is in agreement with previous studies in CHO-K1 cells (20).

According to the simulations and the functional experiments both the antagonists and receptors could be put in order according to their *apparent competitivity* (Table 3). Also the dissociation rate of atropine could be qualitatively predicted although its dissociation rate could not be directly determined (Table 3).

DISCUSSION

The results of the present study demonstrate that the dissociation rate of an antagonist has profound effects on the mode of inhibition of agonist-stimulated Ca^{2+} mobilization. Differences between receptor subtypes as well as antagonists with respect to the apparent *competitivity-noncompetitivity* were seen. Binding experiments show that no true noncompetitivity of interaction takes place at the receptor; therefore the interactions could be called pseudo-noncompetitive, as suggested by El-Fakahany et al. (2). Although it has been suggested earlier as one of the possibilities that the dissociation rate of the antagonist may describe the pseudo-noncompetitive effects (1) very little has been done to prove this in practice or even in theory. The simulations performed demonstrate that the differences in antagonist dissociation rates are sufficient to explain this phenomenon. In addition to the previously described apparent modes of inhibition, i.e. *competitive* and *noncompetitive inhibition*, a novel apparent type of inhibition–*partial noncompetitive inhibition*– was found both in the simulations and in the experiments.

SH-SY5Y human neuroblastoma cells, which express M_1 and M_3 receptors, have been observed to display higher K_i'/K_i'-ratios for antagonists as compared to IMR-32 human neuroblastoma cells which express only M_1 (7). An overall higher degree of apparent *competitivity* in M_3 receptors than in M_1 receptors was thus suggested (7). The result of the present study agree well with these data with respect to atropine. The Ca^{2+} elevations in Sf9 cells are relatively slow and long-lasting as compared to the rapid and transient responses in neuronal cells like SH-SY5Y. A slow dissociation rate would have a much more profound effect in a fast responding system (see also (10)). This could also be

TABLE 2

Rate Constants of Receptor-Radioligand-Complex Dissociation (k_{off}) and the Corresponding Dissociation Half-Times ($t_{1/2}$)

	k_{off} (s^{-1}) or $t_{1/2}$ (min) Receptor		
Radioligand	M_1	M_3	M_5
[^{3}H]NMS	$0.58 \pm 0.15 \times 10^{-3}$ s^{-1} 19.6 ± 5.1 min	$0.52 \pm 0.03 \times 10^{-3}$ s^{-1} 22.2 ± 1.3 min	$0.20 \pm 0.03 \times 10^{-3}$ s^{-1} 55.0 ± 10.7 min
[^{3}H]4-DAMP	$11 \pm 2 \times 10^{-3}$ s^{-1} 1.05 ± 0.19 min	$14 \pm 2 \times 10^{-3}$ s^{-1} 0.825 ± 0.119 min	$2.6 \pm 0.5 \times 10^{-3}$ s^{-1} 4.44 ± 0.87 min

Note. The values are mean ± SEM of 3 determinations in triplicate.

seen in the simulations; if k_2-which essentially governs the rate of response decay-was increased, antagonists had to dissociate much faster to display apparent competitive inhibition (data not shown). Therefore even 4-DAMP displays some pseudo-noncompetitive effect in SH-SY5Y neuroblastoma cells.

One of the central questions in studies on receptor function is how the signals are transmitted to the cell. The current models use assumptions of a steady-state situation to describe the receptor activation-effector coupling (11). It should, however, become increasingly evident from the results such as those shown in the present study that there is a need for dynamic receptor models. It can even be argued on the theoretical basis that steady-state models will not describe most of the physiological signals due to agonist metabolism, GTPase activity of G proteins, changes in agonist affinity due to guanylyl nucleotide binding, feedback regulation such as receptor kinases, etc. We have therefore used the more flexible-and in our opinion more useful-of the two dynamic receptor models, the receptor-inactivation model (15, 16, the other is the rate theory 17), to simulate the receptor behaviour. This model gives relatively realistic values although it is also obvious that all the signal decay features cannot be ascribed to the receptor alone but a more complex model including a simplified signalling cascade will also be required. In our simulations a 30-fold change in dissociation constant was required for each simulated pattern to emerge whereas the measured values were of the order 3-5 times. This suggests that in reality the response may consist of several nonlinear amplification steps, the kinetics of which cannot be determined experimentally at the present (21). The stochiometry of R-G-E coupling suggest a several-fold amplification downstream at each coupling step (21). The Ca^{2+} response itself can be amplified by Ca^{2+} activation of phospholipase Cβ (reviewed in 22) and stimulation of IP_3 receptor function (23, 24, reviewed in 25). In the development of new receptor models the pseudo-noncompetitive inhibition is a tool of great value as it is governed by the easily measured dissociation rate, and any deviation in the real situation from the one predicted by the model suggests a further complexity of the signalling cascade.

TABLE 3

The Order of Apparent Competitivity for the Muscarinic Receptor Subtypes and Antagonists Studied Suggested by the Experiments and the Simulations

Antagonist or receptor subtype	The order of apparent competitivity
4-DAMP	$M_1 \approx M_3 \approx M_5$
Atropine	$M_3 > M_1 \approx M_5$
NMS	$M_1 \approx M_3 > M_5$
M_1	4-DAMP > atropine ≈ NMS
M_3	4-DAMP ≈ atropine > NMS
M_5	4-DAMP > atropine > NMS

ACKNOWLEDGMENTS

This study was funded by The Academy of Finland, The Sigrid Jusélius Foundation, The Borg Foundation, The Magnus Ehrnrooth Foundation and The Oskar Öflund Foundation.

REFERENCES

1. Rang, H. P. (1966) *Proc. R. Soc. Lond. B Biol. Sci.* **164,** 488–510.
2. El-Fakahany, E. E., Surichamorn, W., Amrhein, C. L., Stenstrom, S., Cioffi, C. L., Richelson, E., and McKinney, M. (1988) *J. Pharmacol. Exp. Ther.* **247,** 934–940.
3. Kachur, J. F., Allbee, W. E., and Gaginella, T. S. (1988) *J. Pharmacol. Exp. Ther.* **245,** 455–459.
4. Kenakin, T. P., and Boselli, C. (1990) *Eur. J. Pharmacol.* **191,** 39–48.
5. Patscheke, H. (1990) *Stroke* **21,** IV139–142.
6. Minneman, K. P., and Atkinson, B. (1991) *Mol. Pharmacol.* **40,** 523–530.
7. Kukkonen, J., and Åkerman, K. E. O. (1992) *Biochem. Biophys. Res. Commun.* **189,** 919–924.
8. Vigne, P., Breittmayer, J. P., and Frelin, C. (1993) *Eur. J. Pharmacol.* **245,** 229–232.
9. Sakamoto, A., Yanagisawa, M., Tsujimoto, G., Nakao, K., Toyo

oka, T., and Masaki, T. (1994) *Biochem. Biophys. Res. Commun.* **200,** 679–686.

10. Kukkonen, J. P., Huifang, G., Jansson, C. C., Wurster, S., Cockcroft, V., Savola, J. M., and Åkerman, K. E. O. (1997) *Eur. J. Pharmacol.* **335,** 99–105.
11. Kenakin, T. (1993) Pharmacologic Analysis of Drug-Receptor Interaction, Raven Press, New York.
12. Kukkonen, J. P., Näsman, J., Ojala, P., Oker-Blom, C., and Åkerman, K. E. O. (1996) *J. Pharmacol. Exp. Ther.* **279,** 593–601.
13. Peterson, G. L. (1983) *Methods Enzymol.* **91,** 95–119.
14. Cornish Bowden, A. (1974) *Biochem. J.* **137,** 143–144.
15. Gosselin, R. E. (1970) *Br J Pharmacol* **39,** 215P.
16. Gosselin, R. E. (1977) *in* Kinetics of Drug Action (van Rossum, J. M., Ed.), Vol. 33, pp. 283–335, Springer-Verlag, Berlin.
17. Paton, W. D. M. (1961) *Proc Roy Soc Lond B* **154,** 21–69.
18. Mendes, P. (1993) *Comput. Appl. Biosci.* **9,** 563–571.
19. Hu, Y., Rajan, L., and Schilling, W. P. (1994) *Am. J. Physiol.* **266,** C1736–1743.
20. Ellis, J., Huyler, J., and Brann, M. R. (1991) *Biochem. Pharmacol.* **42,** 1927–1932.
21. Taylor, C. W. (1990) *Biochem. J.* **272,** 1–13.
22. Lee, S. B., and Rhee, S. G. (1995) *Curr. Opin. Cell Biol.* **7,** 183–189.
23. Bezprozvanny, I., Watras, J., and Ehrlich, B. E. (1991) *Nature* **351,** 751–754.
24. Bootman, M. D., Missiaen, L., Parys, J. B., De Smedt, H., and Casteels, R. (1995) *Biochem. J.* **306,** 445–451.
25. Miyazaki, S. (1995) *Curr. Opin. Cell Biol.* **7,** 190–196.